Available online at www.sciencedirect.com
SCIENCE DIRECT®
Journal of Power Sources 124 (2003) 420–425
JOURNAL OF POWER SOURCES
www.elsevier.com/locate/jpowsour

Short communication

Bimetallic Pt–Ru nanowire network for anode material in a direct-methanol fuel cell

Won Choon Choi, Seong Ihl Woo*

Department of Chemical and Biomolecular Engineering, Center for Ultramicrochemical Process Systems, Korea Advanced Institute of Science and Technology, 373-1 Kusong-dong, Yusong-gu, Taejon 305-701, South Korea

Received 30 April 2003; accepted 30 June 2003

Abstract

A new bimetallic nanostructured Pt–Ru material is synthesized in an SBA-15 nanoreactor and compared with commercial Pt–Ru black (Johnson Matthey). Transmission electron microscopic and X-ray diffraction studies of the synthesized material show that, as with a network structure, the Pt–Ru nanowires are interconnected via smaller ones. The catalytic activity (measured in cyclic voltammetry (CV) experiments) for methanol electro-oxidation on the material is lower than that for commercial Pt–Ru black at potentials below 550 mV versus the reversible hydrogen electrode. By contrast, a direct-methanol fuel cell (DMFC) in which the nanostructured material is used as an anode material shows higher performance than with Pt–Ru black, because the network structure leads to an effective mass transfer in the membrane–electrode assembly.

Keywords: Nanowire; Fuel cell; Platinum–rhuthenium; Methanol electro-oxidation; Mass transfer; Membrane–electrode assembly

1. Introduction

In a direct-methanol fuel cell (DMFC), high surface area Pt–Ru blacks have generally been used as an electrocatalyst [1–3]. Current densities in the fuel cell do not, however, scale with intrinsic surface areas and metal loadings. This problem is compounded by the use of polymeric binders for incorporating the Pt–Ru black powders into the desired electrode geometry [4]. Because this hindrance results mainly from the ineffective mass transfer and diffusion in a thick electrode layer that has numerous interfaces between randomly-shaped fine nanoparticles and polymeric binders, a three-dimensional Pt–Ru nanostructured material can be used as a new electrocatalyst for enhancing the performance of DMFCs.

As a method for synthesizing nanostructured materials, replication has been the mainstay for moulding novel material that is synthesized with various lengths and shapes in a removable template [5–7]. For example, monometallic Pt, Au and Ag nanowires [8–11] and Pt nanowire network [12] synthesized in highly ordered SBA-15 silica have been reported. In addition, Ichikawa and co-workers [13,14] have prepared Pt–Rh and Pt–Pd nanowires. As these bimetallic structures were synthesized in FSM-16 or HMM-1, however, no network could be obtained. In this study, a bimetallic Pt–Ru nanowire network is synthesized in a SBA-15 template, as shown in Fig. 1, and its application as a novel electrocatalyst for DMFC is examined.

2. Experimental

SBA-15 silica was prepared using triblock copolymer Pluronic P123 ($EO_{20}PO_{70}EO_{20}$, BASF) and tetraethyl orthosilicate (98%, Aldrich) according to the procedure described elsewhere [15]. In a typical synthesis, as shown in Fig. 1, calcined SBA-15 silica was immersed in an aqueous EtOH–H_2O (1:1 (v/v)) solution that contained $(NH_3)_4Pt(NO_3)_2$ and $(NH_3)_6RuCl_3$ (Pt:Ru = 3:1, atomic ratio). The resulting slurry was dried in a rotary evaporator and the procedure was repeated 10 times for the content of Pt and Ru to become 70 wt.% of SBA-15. After drying the sample in a vacuum oven at 60 °C, it was slurried in CH_2Cl_2 and dried at room temperature to introduce the Pt and Ru precursors on the outer surface of SBA-15 into the silica channels [16]. A careful thermal reduction procedure is required, because the presence of H_2O in a SBA-15

* Corresponding author. Tel.: +82-42-869-3918; fax: +82-42-869-3910.
E-mail address: siwoo@mail.kaist.ac.kr (S.I. Woo).

0378-7753/$ – see front matter © 2003 Elsevier B.V. All rights reserved.
doi:10.1016/S0378-7753(03)00812-7

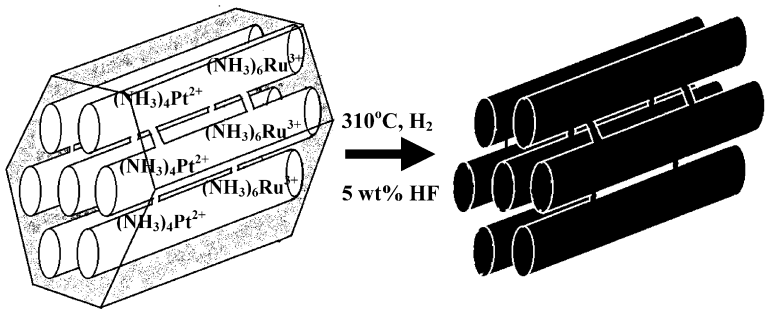

Fig. 1. Schematic of Pt–Ru nanowire network synthesized with a SBA-15 template nanoreactor.

template increases the mobility of the metal precursors in the silica channel [17]. The Pt and Ru species in SBA-15 was reduced by a hydrogen flow while the temperature was increased from room temperature to 310 °C for 6 h. This temperature was maintained for 2 h, and then the hydrogen was evacuated at 310 °C for 30 min. Furthermore, during the heating stage, the temperature was maintained at 100 °C for 1 h. The silica framework of the sample was dissolved completely with 5% hydrofluoric acid. The resulting Pt–Ru was filtered, washed and dried in a vacuum oven at room temperature. The sample synthesized by this procedure is abbreviated as Pt–Ru-NW.

Surface areas were measured by the N_2-BET method using a Micromeritics ASAP2010 instrument. X-ray powder diffraction patterns of the prepared sample were recorded in the small and wide 2θ range by means of a X-ray diffractometer (Rigaku D/MAX-III). Transmission electron microscopy (TEM) was performed on a Philips CM20 instrument with an accelerating voltage of 150 kV. Fourier transformed infrared (FTIR) spectra of CO adsorbed on the pelletized samples were obtained with a Nicolet magna 560 instrument.

Cyclic voltammetry (CV) was conducted to elucidate the adsorption properties of the samples. In order to prepare the modified thin-film electrode, nanowires were dispersed ultrasonically in water at a concentration of 4 mg ml^{-1} and a 20 μl aliquot was transferred on to a polished glassy-carbon substrate. After evaporation of water, the resulting thin catalyst film was covered with 5 wt.% Nafion solution and used as a working electrode. Electrochemical measurements were performed at room temperature in 1 M $HClO_4$, which had been purged with argon for at least 30 min. The scan rate was 15 mV s^{-1}. The reference electrode was a Ag/AgCl electrode, and the counter electrode was a long platinum wire. Stripping CVs of chemisorbed CO were also obtained after elimination of the CO in electrolyte solution by argon bubbling under potential control. The CO was adsorbed for 10 min at a constant electrode potential of 0.1 V. Methanol electro-oxidation in 1 M $HClO_4$/2 M methanol was performed potentiostatically.

DMFC current–voltage curves were obtained using Pt–Ru nanostructured materials as the anode catalyst and Pt black (Johnson Matthey, Hispec 1000) as the cathode catalyst. The loadings of both the anode and cathode catalysts were approximately 5 mg cm^{-2}. The membrane electrode assemblies (MEAs) were prepared by painting the ink-like catalyst slurry on to a carbon diffusion layer and hot-pressing Nafion 117 membrane placed between anode and cathode at 120 °C for 2 min. Two molar methanol (2 cc min^{-1}, 0 psig) and oxygen (500 ml min^{-1}, 0 psig) were delivered to the anode and cathode compartment, respectively.

3. Results and discussion

3.1. Characterization of Pt–Ru nanowire network

As shown in Fig. 2(a), the prepared silica template gives an XRD pattern of a highly ordered SBA-15 sample with a hexagonal structure. As shown in Fig. 2(b), the mesoscopic ordering of SBA-15 is maintained after H_2 reduction of $(NH_3)_4Pt(NO_3)_2$ and $(NH_3)_6RuCl_3$ inside the SBA-15 structure, as indicated by the low-angle peaks of (1 0 0), (1 1 0) and (2 0 0) reflections. No significant structural changes appear in the silica templates after metal loading, except for

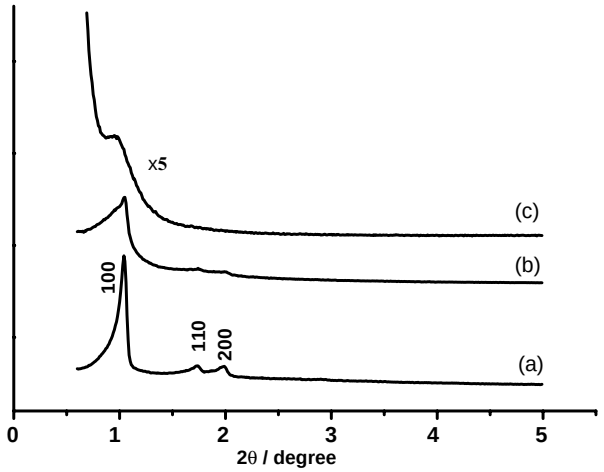

Fig. 2. X-ray diffraction patterns of: (a) SBA-15; (b) Pt–Ru-NW/SBA-15 composite and (c) Pt–Ru-NW obtained after removing SBA-15 from Pt–Ru-NW/SBA-15.

a decrease in peak intensity. By contrast, the XRD pattern of Pt–Ru-NW (Fig. 1(c)) only shows the (1 0 0) reflection because this material does not fill the entire pore volume of the SBA-15 and the as-synthesized Pt–Ru-NW is not sufficiently long to show the whole negatives of the template. The length of nanowires, which are interconnected with each other, can be controlled by the amount of metal loading.

Images taken with transmission electron microscopy show that the length of the nanowires varies from 70 to 200 nm (Fig. 3(a)). Although the samples for the TEM images were prepared after sonicating a small amount of the material in ethanol, the nanowires are not scattered. Other high-resolution TEM images taken with the incident electron beam perpendicular and parallel to the length direction are presented in Fig. 3(b) and (c), respectively. Bridges are observed between nanowires of 7–8 nm in diameter. The direction of the lattice fringe of the nanowires, as shown by arrows in Fig. 3(b), is the same as that of bridges. Therefore, the XRD data and TEM images imply that Pt–Ru-NW should have a Pt–Ru nanowire network structure (v.i.).

Nanostructured platinum, denoted as Pt-NW, was prepared in the same manner as Pt–Ru-NW. The high-angle diffraction peaks of Pt–Ru-NW and Pt-NW are shown in Fig. 4(a) and (b), respectively. The lattice parameters of Pt–Ru-NW and Pt-NW are calculated to be 3.9166 and 3.9204 Å, respectively. The available literature [18], which reports values for the composition in atomic percentage and lattice parameters of Pt–Ru alloy specimens, shows that the lattice parameter of Pt–Ru alloy with 90.3 at.% Pt is 3.9166. Considering that the at.% of platinum of Pt–Ru-NW is 81.1, which is confirmed by an ICP result, 46% of the total Ru atoms are alloyed with Pt and the remaining Ru atoms are present as a hexagonal close-packed phase. Therefore, the XRD pattern for Pt–Ru-NW shows a single fcc phase and small detectable amounts of any other crystalline phases such as hexagonal close-packed Ru, which is indicated by a circle. Because Pt is a well-known catalyst for hydrogenation reactions [19], it is suggested that in the reduction procedure Ru adatoms are evenly deposited on Pt by using the reaction between the small Pt agglomerates and $(NH_3)_6RuCl_3$ in the SBA-15 nanoreactor. This suggests that the as-synthesized Pt–Ru-NW is a well-defined Pt–Ru bimetallic nanowire network, and that a Pt–Ru alloy phase can be prepared at a low reduction temperature.

The binding energy of the Pt $4f_{7/2}$ peak and the Ru $3d_{5/2}$ peak of Pt–Ru-NW is 71.1 and 280.2 eV, respectively. If any electron transfer occurs in the Pt–Ru alloy phase, the binding energy of the platinum in Pt–Ru-NW is expected to be shifted. The observed shift (−0.1 eV) is, however, insufficient to assess the electron transfer. The FTIR spectra of CO adsorbed on Pt–Ru-NW and Pt-NW are shown in Fig. 5(a) and (b), respectively. The linear CO stretching vibration of Pt–Ru-NW appears at 2074 cm^{-1}, while that of Pt-NW appears at 2092 cm^{-1}. The shift in the CO stretching band of the Pt–Ru-NW is attributed to electron transfer from Ru to Pt in the Pt–Ru alloy, which can be explained

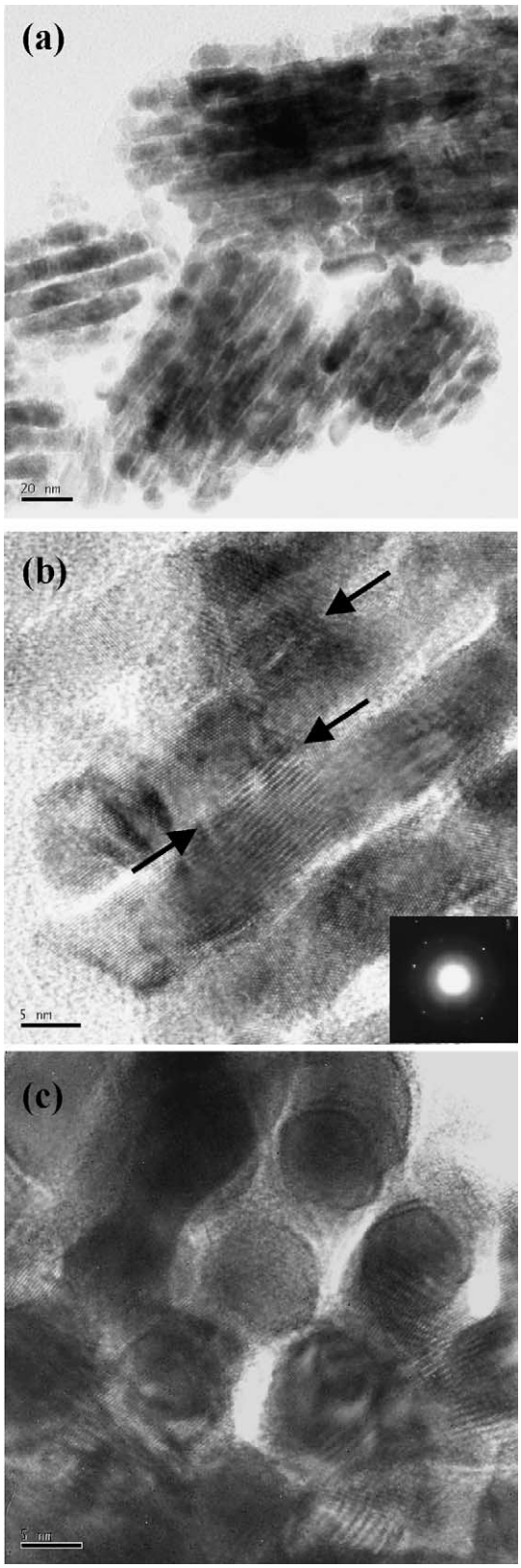

Fig. 3. Bright field: (a) TEM image of Pt–Ru-NW and HRTEM images taken with incident electron beam; (b) perpendicular and (c) parallel to the length direction. A selected area of the electron diffraction pattern of Pt–Ru-NW is shown in inset of (b).

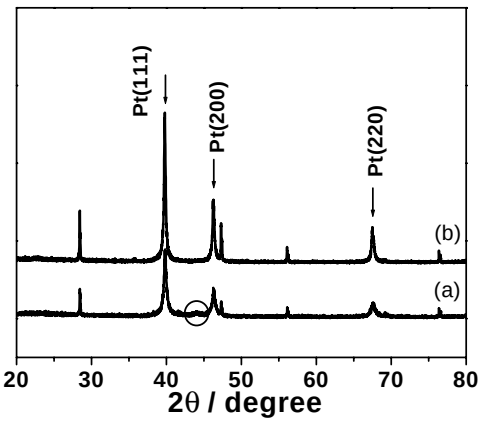

Fig. 4. X-ray diffraction patterns of: (a) Pt–Ru-NW and (b) Pt-NW at high diffraction angle. Small sharp lines except for fcc peaks are from Si standard.

in terms of back donation of electrons from the Pt d-bands into the $2\pi^*$ molecular orbital of the adsorbed CO. This result agrees with the finding of Goodenough et al. [20]. By contrast, McBreen and Mukerjee [21] used X-ray absorption spectroscopy to show that Pt alloyed with Ru causes an increase in the number of Pt d-band vacancies.

3.2. Electrochemical studies

CO stripping experiments for evaluating the amount of adsorbed CO were performed to measure the electrochemically active area. Typical CVs for CO oxidation are in Fig. 6. Due to the strong adsorption of CO on the Pt surface, hydrogen adsorption–desoption on Pt is completely blocked in the hydrogen region; this indicates the presence of a saturated CO adlayer. The electrochemical surface area was measured by CO stripping, assuming an adsorption charge of 420 $\mu C\,cm^{-2}$ Pt for a CO monolayer. The values for Pt–Ru-NW and a commercial Pt–Ru black (Johnson Matthey, Hispec 6000) are 1.27 and 2.1 cm^2 Pt/cm^2 thin-film electrode, respectively. Considering the BET surface area of the commercial Pt–Ru black is 1.5 times higher than that of Pt–Ru-NW, nanopores between Pt–Ru nanowires and an enriched Pt surface of Pt–Ru-NW may result in the increase in the electrochemical surface area of this material.

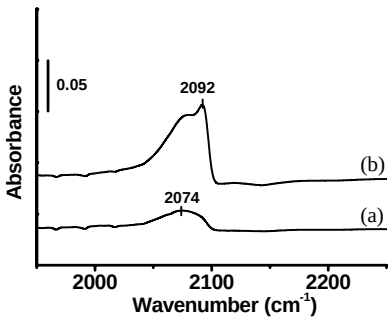

Fig. 5. FTIR spectra of CO adsorbed on: (a) Pt–Ru-NW and (b) Pt-NW.

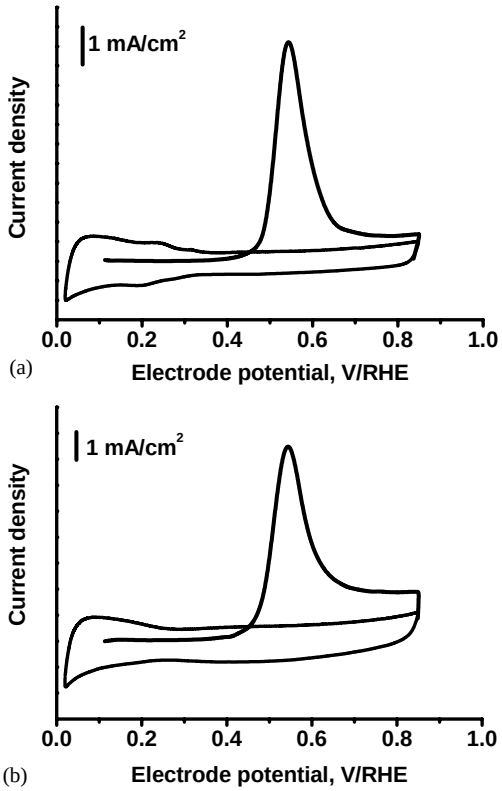

Fig. 6. Steady-state cyclic voltammograms of: (a) Pt–Ru-NW and (b) commercial Pt–Ru black electrode for oxidation of monolayer-adsorbed carbon monoxide at 15 mV s^{-1} scan rate.

Since CO_{ads} is postulated to be an intermediate in methanol electro-oxidation on Pt surfaces and to decrease the number of active sites [22], oxidizing the CO adsorbed on Pt to CO_2 is important in enhancing the electrocatalytic activity of Pt. The electrocatalytic activities for the methanol electro-oxidation (Eq. (1)) of Pt–Ru-NW and commercial Pt–Ru black (Pt/Ru = 1, Johnson Matthey), are shown in Fig. 6(a).

$$CH_3OH + H_2O \rightarrow CO_2 + 6H^+ + 6e^- \quad (1)$$

At low potentials, rate-limiting step of this reaction involves the formation of oxidatively adsorbed water for the oxidation of CO_{ads} and a Pt:Ru ratio of near unity should be optimal [23,24]. At high potentials, however, where oxidative adsorption of water is facile, a surface Pt:Ru ratio of greater than unity is advantageous to methanol chemisorption [25,26]. As shown in Fig. 7(a), the commercial Pt–Ru black (Pt/Ru = 1) shows a slightly higher activity than the as-synthesized Pt–Ru-NW (Pt/Ru = 4.3) at low potentials ($E < 0.55$ V). On the other hand, Pt–Ru-NW becomes more active than commercial Pt–Ru black at higher potentials ($E > 0.55$ V), but this potential region is not applicable to DMFC operation, for which the anode potential is less than 0.6 V.

Although Pt–Ru-NW does not show higher activity at a potential less than 0.55 V, as shown in Fig. 7(a), it gives a higher DMFC performance than the commercial

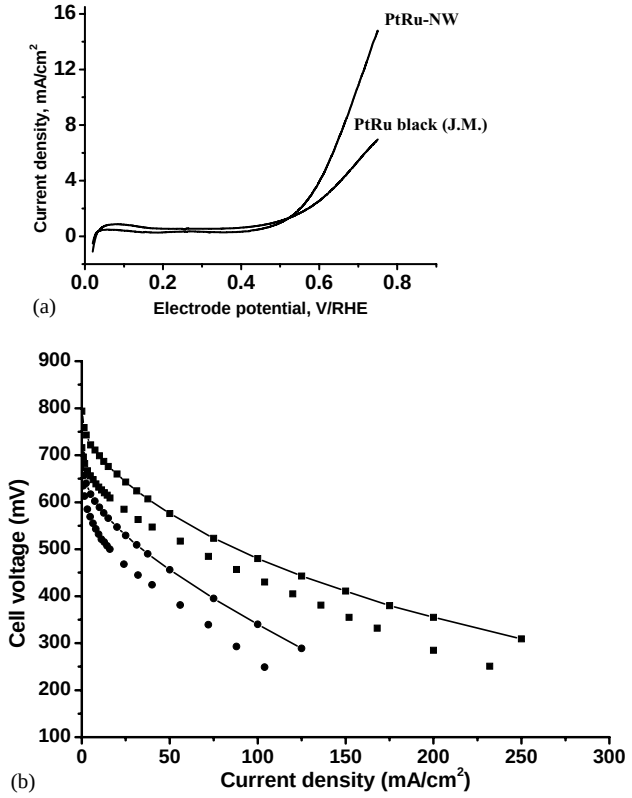

Fig. 7. (a) Cyclic voltammograms on methanol electro-oxidation and (b) DMFC current density–voltage curves at 40 °C (circles) and 80 °C (squares) that compare the performance of Pt–Ru-NW (connected data point) with that of Johnson Matthey commercial Pt–Ru black (unconnected data point) in a single-cell test (catalyst loading: 5 mg cm^{-2}).

Pt–Ru black catalyst, as shown in Fig. 7(b). Many results have been reported for improving the activity of methanol electro-oxidation, and bimetallic Pt–Ru is known to be a good catalyst system. This behaviour has been explained in terms of a bifunctional mechanism and an electronic effect [27–31]. While these two models are mainly considered for thin-film electrodes in half cell experiments with a negligible mass transfer effect, the relative anode performance of a MEA depends strongly on the mass transport of reactants and products, as well as on the electrical conductivity of the catalyst layer and the spillover of protons [2,32]. Consequently, as mentioned in the introduction above, the current density of thin-film electrodes does not appear in a MEA. Compared with a Pt–Ru black with uncontrolled morphology, the application of a three-dimensional Pt–Ru nanowire network as electrode material has some advantages; namely, it reduces the number of interfaces that result from mixing the electrocatalyst and binders, and it uses its mesopores for the effective mass-transport/diffusion of reactants and products. Increasing the content of the PTFE or Nafion binder in the anode renders the morphology more favourable for the efficient CO_2 path [33].

On the other hand, the low electrical conductivity of binders and the resulting thick electrode decrease the performance of DMFCs. Therefore, it is more desirable to prepare an electrode with effective morphology without increasing the binder content. Synthesis of a mesoporous electrocatalyst can be a good way to do this.

4. Conclusions

Optimizing the structure of an electrode layer for effective mass transfer and high electrocatalytic activity is crucial for enhancing the performance of fuel cells, as well as for reducing the amount of expensive electrocatalyst. Such control can be achieved by synthesizing a nanostructured electrocatalyst. To demonstrate this concept, a bimetallic Pt–Ru nanowire network has been synthesized. This employs a catalytic reaction between surface platinum and a ruthenium-ammine compound in a SBA-15 template nanoreactor. The resulting Pt–Ru-NW nanowire network when used as an anode material improves the performance of a DMFC significantly. Furthermore, by using silica templates with various wall thicknesses and pore diameters [34], the structure of the nanowire network can be controlled in order to find the most efficient electrode material.

Acknowledgements

This research was funded by the Center for Ultramicrochemical Process Systems sponsored by KOSEF. The authors are also grateful for partial financial support from ITEP Samsung Advanced Institute of Technology, LG Chem., Korea Storage Battery, Haesong P&C, and Hankook Tire.

References

[1] X. Ren, M. S. Wilson, S. Gottesfeld, J. Electrochem. Soc. 143 (1996) L12.
[2] A. S. Aricò, A. K. Shukla, K. M. El-Khatib, P. Cretì, V. Antonucci, J. Appl. Electrochem. 29 (1999) 671.
[3] L. Liu, C. Pu, R. Viswanathan, Q. Fan, R. Liu, E. S. Smotkin, Electrochim. Acta 43 (1998) 3657.
[4] M. L. Anderson, R. M. Stroud, D. R. Rolison, Nano Lett. 2 (2002) 235.
[5] S. Mann, G. A. Ozin, Nature 382 (1996) 313.
[6] G. L. Egan, J. Yu, C. H. Kim, S. J. Lee, R. E. Schaak, T. E. Mallouk, Adv. Mater. 12 (2000) 1040.
[7] H. J. Shin, R. Ryoo, Z. Liu, O. Terasaki, J. Am. Chem. Soc. 123 (2001) 1246.
[8] R. Ryoo, C. H. Ko, M. Kruk, V. Antochshuk, M. Jaroniec, J. Phys. Chem. B 104 (2000) 11465.
[9] Y. Han, J. M. Kim, G. D. Stucky, Chem. Mater. 12 (2000) 2068.
[10] Z. Liu, O. Terasaki, T. Ohsuna, K. Hiraga, H. J. Shin, R. Ryoo, Chem. Phys. Chem. 2 (2001) 229.
[11] M.H. Huang, A. Choudrey, P. Yang, Chem. Commun. (2000) 1063.
[12] H. J. Shin, C. H. Ko, R. Ryoo, J. Mater. Chem. 11 (2001) 260.
[13] A. Fukuoka, Y. Sakamoto, S. Guan, S. Inagaki, N. Sugimoto, Y. Fukushima, K. Hirahara, S. Iijima, M. Ichikawa, J. Am. Chem. Soc. 123 (2001) 3373.
[14] A. Fukuoka, N. Higashimoto, Y. Sakamoto, S. Inagaki, Y. Fukushima, M. Ichikawa, Micropor. Mesopor. Mater. 48 (2001) 171.

[15] D. Zhao, J. Feng, Q. Huo, N. Melosh, G. H. Fredrickson, B. F. Chmelka, G. D. Stucky, Science 279 (1998) 548.
[16] Y. Han, J. M. Kim, G. D. Stucky, Chem. Mater. 12 (2000) 2068.
[17] H. J. Shin, R. Ryoo, Z. Liu, O. Terasaki, J. Am. Chem. Soc. 123 (2001) 3373.
[18] H. A. Gasteiger, P.N. Ross Jr., E. J. Cairns, Surf. Sci. 293 (1993) 67.
[19] C. E. Lee, S. H. J. Bergens, Phys. Chem. B 102 (1998) 193.
[20] J. B. Goodenough, R. Manoharan, A. K. Shukia, K. V. Ramesh, Chem. Mater. 1 (1989) 391.
[21] J. McBreen, S. Mukerjee, J. Electrochem. Soc. 142 (1995) 3399.
[22] W. C. Choi, J. D. Kim, S. I. Woo, Catal. Today 74 (2002) 235.
[23] P. S. Kauranen, E. Skou, J. Munk, J. Electroanal. Chem. 404 (1996) 1.
[24] R. Liu, H. Iddir, Q. Fan, G. Hou, A. Bo, K. L. Ley, E. S. Smotkin, Y. Sung, H. Kim, S. Thomas, A. Wieckowski, J. Phys. Chem. B 104 (2000) 3518.
[25] H. A. Gasteiger, N. Markovic, P.N. Ross Jr., E. J. Cairns, J. Phys. Chem. 97 (1993) 12020.
[26] H. A. Gasteiger, N. Markovic, P.N. Ross Jr., E. J. Cairns, J. Electrochem. Soc. 141 (1994) 1795.
[27] M. Watanabe, S. J. Motoo, Electoanal. Chem. 60 (1975) 283.
[28] E. Ticianelli, J. G. Beery, M. T. Paffett, S. Gottesfeld, J. Electroanal. Chem. 258 (1989) 61.
[29] M. Krausa, W. Vielstich, J. Electroanal. Chem. 379 (1994) 307.
[30] J. B. Goodenough, A. Hamnett, B. J. Kennedy, R. Manoharan, S. A. Weeks, J. Electroanal. Chem. 240 (1988) 133.
[31] C. Liu, C. Rice, R. I. Masel, P. K. Babu, P. Waszczuk, H. S. Kim, E. Oldfield, A. Wieckowski, J. Phys. Chem. B 106 (2002) 9581.
[32] E. S. Steigerwalt, G. A. Deluga, C. M. Lukehart, J. Phys. Chem. B 106 (2002) 760.
[33] J. Nordlund, A. Roessler, G. Lindbergh, J. Appl. Electrochem. 32 (2002) 259.
[34] J. -S. Lee, S. H. Joo, R. Ryoo, J. Am. Chem. Soc. 124 (2002) 1156.